

Optical response of a dissipative optomechanical system with a weak mechanical driveSumei Huang ¹, Li Deng,² and Aixi Chen ^{1,*}¹*Key Laboratory of Optical Field Manipulation of Zhejiang Province, Department of Physics, Zhejiang Sci-Tech University, Hangzhou 310018, China*²*School of Science, Zhejiang Sci-Tech University, Hangzhou 310018, China*

(Received 22 December 2023; accepted 29 April 2024; published 15 May 2024)

We study the propagation of a weak probe field through a dissipative optomechanical system, in which an additional weak mechanical drive is acting directly on a vibrating waveguide. In the presence of a strong coupling field, when the frequency of the mechanical drive precisely matches the frequency difference between the probe and coupling fields, we show that the nearly perfect absorption, complete transmission, and significant amplification of the probe field can be achieved by adjusting the amplitude and phase of the mechanical drive and the power of the coupling field. Moreover, by appropriately choosing the amplitude and phase of the mechanical drive, the group delay of the output probe field is tunable from a large negative value to a large positive value and vice versa. Our study offers an alternative way to control and manipulate the propagation of a weak probe field in a dissipative optomechanical system.

DOI: [10.1103/PhysRevA.109.053517](https://doi.org/10.1103/PhysRevA.109.053517)**I. INTRODUCTION**

Cavity optomechanics has made rapid progress in recent years and played an important role in quantum information processing [1]. In a dispersive optomechanical system, a single-mode cavity field exerts a radiation pressure force on a macroscopic mechanical oscillator, and the motion of the mechanical oscillator changes the cavity resonance frequency [1]. Recently, the electromagnetically induced transparency (EIT) was demonstrated in a dispersive optomechanical system in both theory [2] and experiment [3–6]. The EIT was first observed in three-level atomic systems [7–9]. It is an unusual phenomenon in which a strong coupling field makes an opaque atomic system transparent to a weak probe field in a narrow range of frequencies due to the destructive interference between the probability amplitudes associated with two excitation pathways [7–9]. In contrast, the electromagnetically induced absorption (EIA) is a coherent phenomenon due to the constructive interference between the probability amplitudes associated with two excitation pathways in atomic systems [10]. The EIA was reported in a dispersive optomechanical system experimentally [4,11] and theoretically [12]. In addition, the electromagnetically induced amplification was demonstrated in a dispersive optomechanical system experimentally [4,6,11]. Meanwhile, it has been reported that the EIT is accompanied by a rapid change in the phase of the output probe field, which leads to a positive or negative group delay of the output probe field, thereby producing slow light or fast light [4,5]. The slow light has potential applications in optical buffering [4] and light storage [13].

Besides the dispersive optomechanical system, there exists a dissipative optomechanical system, in which a single-mode

cavity field exerts a reactive optical force on a macroscopic mechanical oscillator, and the motion of the mechanical oscillator changes the external decay rate of the cavity field [14,15]. The dissipative optomechanical coupling exists in several different experimental setups [15–18], such as a microdisk cavity coupled to a vibrating waveguide [15], a Michelson-Sagnac interferometer with a vibrating membrane [16], a nanometer-scale carbon nanotube coupled to a micrometer-scale optical cavity [17], and a pair of identical silicon photonic crystal nanobeams [18]. Recently, theoretical analysis and experimental observations have demonstrated that the dissipative optomechanical coupling can cool a mechanical oscillator to near its quantum ground state in the unresolved-sideband limit [16,19–22]. The cooling of the mechanical oscillator offers the possibility to observe many physical phenomena in such a system, such as high-precision sensors [23,24], self-oscillation in the red detuning regime [25], squeezed light [26–29], mechanical squeezing [30,31], normal mode splitting in the output fields [32,33], and EIT phenomenon [18,33]. In Ref. [25], it has been reported that the self-oscillation in the red detuning regime is due to the anti-damping effects of dissipative optomechanical coupling on the mechanical oscillator, and the transmission of the cavity field is affected by the vertical offset of the mechanical oscillator in the presence of the dissipative optomechanical coupling. In Ref. [33], the existence of EIT in the output probe field in a dissipative optomechanical system in the presence of a strong coupling field has been shown, and the EIT peak becomes wider for a larger power of the coupling field.

Recent studies have shown that the optical response of a dispersive optomechanical system can be modified by an additional mechanical field acting on a mechanical oscillator [34–37]. In a linearly coupled dispersive optomechanical system with a weak mechanical pump [34,35], it has been found that the nearly perfect absorption, transparency, and ampli-

*aixichen@zstu.edu.cn

fication of a weak probe field can be achieved by adjusting the amplitude and phase of a weak mechanical pump and the effective optomechanical coupling strength [34,35], and the group delay of the output probe field can be changed from $-20 \mu\text{s}$ to $20 \mu\text{s}$ by varying the amplitude of the weak mechanical pump [35]. Moreover, in a multimode linearly coupled dispersive optomechanical system [36], which is formed by a cavity mode and two coupled mechanical modes with different frequencies, and where the high-frequency mechanical mode is driven by a mechanical pump, it has been shown that a cascaded EIT effect can be observed, and the group delay of the output probe field can be changed from $5 \mu\text{s}$ to $-1.03 \mu\text{s}$ by changing the detuning of the mechanical pump acting on the high-frequency mechanical oscillator. It is noted that the group delay $5 \mu\text{s}$ ($-1.03 \mu\text{s}$) corresponds to 5000π (-1030π) times the photon lifetime κ^{-1} in the cavity, where κ is the cavity decay rate and $\kappa = 2\pi \times 0.5 \text{ GHz}$ [36]. In addition, in a quadratically coupled dispersive optomechanical system with a mechanical degenerate parametric drive [37], it has been shown that the opacity and amplification of a weak probe field can be obtained by varying the amplitude and phase of a weak mechanical drive.

In this paper, we study the response of a dissipative optomechanical system to a weak probe field in the presence of a strong coupling field and a weak coherent mechanical drive. We find that a proper choice of the amplitude and phase of the mechanical drive and the power of the coupling field can lead to nearly perfect absorption, full transmission, and amplification of the probe field in both the critical coupling regime and the undercoupling regime. We show that it is possible to observe the EIT-like feature and the EIA-like feature in the intensity of the output probe field. In addition, we show that the group delay of the output probe field can be tuned from a large negative value to a large positive value and vice versa by controlling the amplitude and phase of the mechanical drive.

The remainder of this paper is structured as follows. In Sec. II, we describe the model under investigation, derive the equations of motion for the cavity and mechanical modes, and calculate the output probe field and its group delay. In Sec. III, we discuss the effects of the mechanical drive and the coupling field on the intensity of the output probe field in the purely dissipative optomechanical system. In Sec. IV, we show the influence of the mechanical drive on the group delay of the output probe field in the purely dissipative optomechanical system. In Sec. V, we compare the impacts of the mechanical drive on the intensity and group delay of the output probe field with and without the dispersive coupling. In Sec. VI, we summarize the results.

II. MODEL

The system under consideration consists of a free-standing waveguide and a microdisk [15], as shown in Fig. 1. An intense coupling field with frequency ω_c and a weak probe field with frequency ω_p are sent into the waveguide. The evanescent field from the waveguide is coupled into the microdisk and back through a small gap between them, and a single cavity mode c is generated inside the microdisk. The waveguide is modeled as a damped harmonic oscillator with mass m , resonance frequency ω_m , and damping rate γ_m . The photons

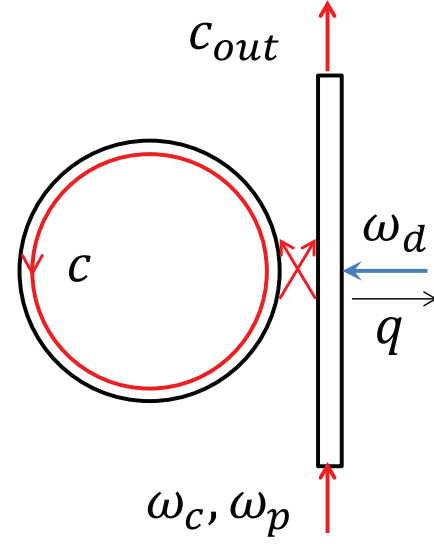


FIG. 1. Sketch of an optomechanical system with a waveguide coupled to a microdisk resonator. An intense coupling field with frequency ω_c and a weak probe field with frequency ω_p are injected into the waveguide, and a single cavity mode c is generated in the microdisk. A weak mechanical pump with frequency ω_d is applied to the waveguide.

from the microdisk cavity exert a radiation pressure force and a reactive optical force on the waveguide, thereby causing it to oscillate. Moreover, a weak coherent mechanical drive with amplitude ε_d , frequency ω_d , and phase ϕ is applied to the waveguide. The weak mechanical drive can be realized by using a piezoelectric drive [36]. The displacement q of the waveguide not only modulates the resonance frequency of the optical cavity mode, denoted by $\omega_0(q)$, but also changes the external decay rate of the cavity field due to the microdisk-waveguide coupling, denoted by $\kappa_e(q)$.

In a frame rotating with the frequency ω_c of the coupling field, the total Hamiltonian of the coupled system can be written as

$$\begin{aligned}
 H = & \hbar[\omega_0(q) - \omega_c]c^\dagger c + \frac{1}{2} \left(m\omega_m^2 q^2 + \frac{p^2}{m} \right) + i\hbar\sqrt{2\kappa_e(q)} \\
 & \times [c^\dagger(\varepsilon_c + \varepsilon_p e^{-i\delta t} + c_{\text{in}}) - c(\varepsilon_c + \varepsilon_p^* e^{i\delta t} + c_{\text{in}}^\dagger)] \\
 & + i\hbar\varepsilon_d(e^{-i\omega_d t - i\phi} b^\dagger - e^{i\omega_d t + i\phi} b), \quad (1)
 \end{aligned}$$

where the first term is the energy of the cavity field in the microdisk; the second term is the center-of-mass energy of the waveguide; the third term describes the couplings of the cavity field with the strong coupling field, the weak probe field, and the incident optical vacuum noise c_{in} ; and the last term represents that the waveguide is driven by a weak mechanical pump. The c and c^\dagger are the annihilation and creation operators of the intracavity photons. The δ is the frequency difference between the probe and coupling fields ($\delta = \omega_p - \omega_c$). The displacement and momentum operators (q , p) of the waveguide can be expressed in terms of the annihilation and creation operators (b , b^\dagger) of the phonons in the waveguide by $q = \sqrt{\frac{\hbar}{2m\omega_m}}(b + b^\dagger)$ and $p = -i\sqrt{\frac{\hbar m\omega_m}{2}}(b - b^\dagger)$. The

amplitudes ε_c and ε_p of the classical coupling and probe fields are proportional to the square root of their respective powers \mathcal{P}_c and \mathcal{P}_p by $\varepsilon_c = \sqrt{\frac{\mathcal{P}_c}{\hbar\omega_c}}$ and $\varepsilon_p = \sqrt{\frac{\mathcal{P}_p}{\hbar\omega_p}}$, respectively. The quantum noise c_{in} has zero mean value. If the displacement q of the waveguide from its equilibrium position is very small, $\omega_0(q)$ and $\kappa_e(q)$ can be approximately expanded to first order in the displacement q of the waveguide,

$$\begin{aligned}\omega_0(q) &\approx \omega_0 + g_{\omega 0}q, \\ \kappa_e(q) &\approx \kappa_e + g_{\kappa 0}q,\end{aligned}\quad (2)$$

where ω_0 and κ_e denote the resonance frequency and the external decay rate of the cavity field when $q = 0$, respectively, and the parameters $g_{\omega 0}$ and $g_{\kappa 0}$ represent the strengths of the dispersive and dissipative optomechanical interactions, respectively. Besides, when the mechanical displacement q is very small, $\sqrt{2\kappa_e(q)}$ can be approximated to first order in q by $\sqrt{2\kappa_e(q)} \approx \sqrt{2\kappa_e}(1 + \frac{g_{\kappa 0}}{2\kappa_e}q)$. We assume $\kappa_e = \eta\kappa$, where κ is the total decay rate of the cavity field ($\kappa = \kappa_e + \kappa_i$), and κ_i is the intrinsic decay rate of the cavity field inside the microdisk. Thus, the Hamiltonian of the system has the form

$$\begin{aligned}H &= \hbar \left[\omega_0 - \omega_c + \frac{g_{\omega}}{\sqrt{2}}(b + b^\dagger) \right] c^\dagger c + \hbar \omega_m \left(b^\dagger b + \frac{1}{2} \right) + i\hbar \sqrt{2\eta\kappa} \left[1 + \frac{g_{\kappa}}{2\sqrt{2}\eta\kappa}(b + b^\dagger) \right] \\ &\times [c^\dagger (\varepsilon_c + \varepsilon_p e^{-i\delta t} + c_{\text{in}}) - c(\varepsilon_c + \varepsilon_p^* e^{i\delta t} + c_{\text{in}}^\dagger)] + i\hbar \varepsilon_d (e^{-i\omega_d t - i\phi} b^\dagger - e^{i\omega_d t + i\phi} b),\end{aligned}\quad (3)$$

where $g_{\omega} = g_{\omega 0}q_{\text{zpf}}$, $g_{\kappa} = g_{\kappa 0}q_{\text{zpf}}$, and $q_{\text{zpf}} = \sqrt{\frac{\hbar}{m\omega_m}}$ is the zero-point fluctuation of the waveguide.

Applying the above Hamiltonian to the Heisenberg equation of motion, we obtain the two coupled first-order differential equations for the operators c and b

$$\begin{aligned}\dot{c} &= - \left\{ \kappa + \frac{g_{\kappa}}{\sqrt{2}}(b + b^\dagger) + i \left[\omega_0 - \omega_c + \frac{g_{\omega}}{\sqrt{2}}(b + b^\dagger) \right] \right\} c + \sqrt{2\eta\kappa} \left[1 + \frac{g_{\kappa}}{2\sqrt{2}\eta\kappa}(b + b^\dagger) \right] (\varepsilon_c + \varepsilon_p e^{-i\delta t} + c_{\text{in}}), \\ \dot{b} &= - \left(\frac{\gamma_m}{2} + i\omega_m \right) b - i \frac{g_{\omega}}{\sqrt{2}} c^\dagger c + \frac{g_{\kappa}}{2\sqrt{\eta\kappa}} [c^\dagger (\varepsilon_c + \varepsilon_p e^{-i\delta t} + c_{\text{in}}) - c(\varepsilon_c + \varepsilon_p^* e^{i\delta t} + c_{\text{in}}^\dagger)] + \varepsilon_d e^{-i\omega_d t - i\phi} + \sqrt{\gamma_m} b_{\text{in}},\end{aligned}\quad (4)$$

where we have included the damping and noise terms, and b_{in} is the annihilation operator of the thermal Brownian noise of the waveguide with zero mean value.

We assume that the coupling field is much stronger than the probe field ($\varepsilon_c \gg \varepsilon_p$), and the amplitude ε_c of the coupling field and the amplitude ε_d of the mechanical drive satisfies $\sqrt{2\eta\kappa}\varepsilon_c \gg \varepsilon_d$. From Eq. (4), we obtain the mean values of the operators c and b at the steady state

$$\begin{aligned}c_s &= \frac{\mu}{\kappa + i\Delta + g_{\kappa}Q_s} \varepsilon_c, \\ b_s &= \frac{\frac{g_{\kappa}}{2\sqrt{\eta\kappa}}(c_s^* - c_s)\varepsilon_c - i\frac{g_{\omega}}{\sqrt{2}}|c_s|^2}{\frac{\gamma_m}{2} + i\omega_m},\end{aligned}\quad (5)$$

where $\mu = \sqrt{2\eta\kappa}(1 + \frac{g_{\kappa}}{2\eta\kappa}Q_s)$, and $\Delta = \omega_0 - \omega_c + g_{\omega}Q_s$ is the effective cavity detuning with respect to the coupling frequency ω_c , depending on the steady-state displacement $Q_s = \frac{1}{\sqrt{2}}(b_s + b_s^*)$ of the waveguide. The c_s and b_s are the steady-state amplitudes of the cavity and mechanical modes, respectively, and they are dependent on each other.

Under the assumptions of $\varepsilon_c \gg \varepsilon_p$ and $\sqrt{2\eta\kappa}\varepsilon_c \gg \varepsilon_d$, the system operators c and b can be expressed as $o = o_s + \delta o$ ($o = c, b$), where δo is the time-dependent fluctuation operator, and is small in comparison with the average value o_s . Thus, the nonlinear equation (4) can be linearized. Only keeping the first order in the small fluctuation operator, we obtain the linearized differential equations for the fluctuation operators δc and δb ,

$$\begin{aligned}\delta\dot{c} &= -(\kappa + g_{\kappa}Q_s + i\Delta)\delta c + A(\delta b + \delta b^\dagger) + \mu(\varepsilon_p e^{-i\delta t} + c_{\text{in}}), \\ \delta\dot{b} &= - \left(\frac{\gamma_m}{2} + i\omega_m \right) \delta b + F^* \delta c^\dagger - F \delta c + \frac{g_{\kappa}}{2\sqrt{\eta\kappa}} [c_s^* (\varepsilon_p e^{-i\delta t} + c_{\text{in}}) - c_s (\varepsilon_p^* e^{i\delta t} + c_{\text{in}}^\dagger)] + \varepsilon_d e^{-i\omega_d t - i\phi} + \sqrt{\gamma_m} b_{\text{in}},\end{aligned}\quad (6)$$

where $A = g_{\kappa}(-\frac{c_s}{\sqrt{2}} + \frac{\varepsilon_c}{2\sqrt{\eta\kappa}}) - i\frac{g_{\omega}c_s}{\sqrt{2}}$, $F = \frac{g_{\kappa}}{2\sqrt{\eta\kappa}}\varepsilon_c + i\frac{g_{\omega}}{\sqrt{2}}c_s^*$. Following the same approach as in Ref. [34], we introduce the slow varying operators defined by $\delta c = \delta\tilde{c}e^{-i\delta t}$, $c_{\text{in}} = \tilde{c}_{\text{in}}e^{-i\delta t}$, $\delta b = \delta\tilde{b}e^{-i\omega_d t}$, and $b_{\text{in}} = \tilde{b}_{\text{in}}e^{-i\omega_d t}$. We assume that the coupling field is red-detuned with respect to the cavity resonance frequency ω_0 by one mechanical resonance frequency ω_m ($\Delta = \omega_m$), and the frequency ω_d of the mechanical drive matches the frequency difference δ between the probe and coupling fields ($\omega_d = \delta$). Meanwhile, we assume that the resonance frequency ω_m of the waveguide is much larger than

$\kappa + g_{\kappa}Q_s$, $|A|$, γ_m , $|F|$, and $|\frac{g_{\kappa}}{2\sqrt{\eta\kappa}}c_s|$. After making the rotating wave approximation to remove the rapidly oscillating terms with $e^{2i\delta t}$, we obtain the equations for the fluctuation operators $\delta\tilde{c}$ and $\delta\tilde{b}$,

$$\begin{aligned}\delta\dot{\tilde{c}} &= -(\kappa + g_{\kappa}Q_s - ix)\delta\tilde{c} + A\delta\tilde{b} + \mu(\varepsilon_p + \tilde{c}_{\text{in}}), \\ \delta\dot{\tilde{b}} &= - \left(\frac{\gamma_m}{2} - ix \right) \delta\tilde{b} - F\delta\tilde{c} + \frac{g_{\kappa}}{2\sqrt{\eta\kappa}}c_s^*(\varepsilon_p + \tilde{c}_{\text{in}}) \\ &\quad + \varepsilon_d e^{-i\phi} + \sqrt{\gamma_m}\tilde{b}_{\text{in}},\end{aligned}\quad (7)$$

where $x = \delta - \omega_m$ is the detuning of the probe field from the cavity resonance frequency. It is noted that both the input vacuum noise \tilde{c}_{in} and the thermal noise \tilde{b}_{in} have zero mean values. Thus, at the steady state, the expectation values of the fluctuation operators $\delta\tilde{c}$ and $\delta\tilde{b}$ are found to be

$$\begin{aligned}\langle\delta\tilde{c}\rangle &= \frac{1}{d(x)}[J(x)\varepsilon_p + A\varepsilon_d e^{-i\phi}], \\ \langle\delta\tilde{b}\rangle &= \frac{1}{\frac{\gamma_m}{2} - ix}[B_1(x)\varepsilon_p + B_2(x)\varepsilon_d e^{-i\phi}],\end{aligned}\quad (8)$$

where $J(x) = A\frac{g_\kappa}{2\sqrt{\eta\kappa}}c_s^* + \mu(\frac{\gamma_m}{2} - ix)$, $d(x) = (\kappa + g_\kappa Q_s - ix)(\frac{\gamma_m}{2} - ix) + AF$, $B_1(x) = -F\frac{J(x)}{d(x)} + \frac{g_\kappa}{2\sqrt{\eta\kappa}}c_s^*$, and $B_2(x) = -F\frac{A}{d(x)} + 1$. Note that the amplitude $\langle\delta\tilde{c}\rangle$ of the cavity excitation and the amplitude $\langle\delta\tilde{b}\rangle$ of the mechanical excitation are oscillating at frequency $\omega_p - \omega_c$ in the rotating frame at the coupling frequency ω_c , respectively.

The output field c_{out} from the cavity is related to the cavity field c through the input-output formalism $c_{\text{out}} = \sqrt{2\kappa_e(q)}c - \varepsilon_c - \varepsilon_p e^{-i\delta t} - c_{\text{in}}$ [38]. Thus, the fluctuation δc_{out} of the output field is given by

$$\delta c_{\text{out}} = \mu\delta c + \frac{g_\kappa}{2\sqrt{\eta\kappa}}(\delta b + \delta b^\dagger)c_s - \varepsilon_p e^{-i\delta t} - c_{\text{in}}. \quad (9)$$

Furthermore, we introduce the slow varying operators defined by $\delta c_{\text{out}} = \delta\tilde{c}_{\text{out}}e^{-i\delta t}$, $\delta c = \delta\tilde{c}e^{-i\delta t}$, $c_{\text{in}} = \tilde{c}_{\text{in}}e^{-i\delta t}$, and $\delta b = \delta\tilde{b}e^{-i\omega_d t}$, and assume $\delta = \omega_d$. After dropping the fast oscillating term which contains $e^{2i\delta t}$, we obtain the expectation value of the fluctuation $\delta\tilde{c}_{\text{out}}$ of the output field at the probe frequency ω_p

$$\begin{aligned}\langle\delta\tilde{c}_{\text{out}}\rangle &= \mu\langle\delta\tilde{c}\rangle + \frac{g_\kappa}{2\sqrt{\eta\kappa}}c_s\langle\delta\tilde{b}\rangle - \varepsilon_p \\ &= \left[\mu\frac{J(x)}{d(x)} + \frac{g_\kappa c_s B_1(x)}{2\sqrt{\eta\kappa}(\frac{\gamma_m}{2} - ix)} - 1 \right] \varepsilon_p \\ &\quad + \left[\mu\frac{A}{d(x)} + \frac{g_\kappa c_s B_2(x)}{2\sqrt{\eta\kappa}(\frac{\gamma_m}{2} - ix)} \right] \varepsilon_d e^{-i\phi}.\end{aligned}\quad (10)$$

The first term in Eq. (10) is the contribution from the regular EIT [18,33]. When the coupling field at frequency ω_c interacts with the mechanical phonons at frequency ω_m , the Stokes and anti-Stokes fields are generated. In the resolved-sideband regime ($\omega_m \gg \kappa$), the Stokes field at frequency $\omega_c - \omega_m$ is highly off-resonant with the cavity field, leading to the strong suppression of the Stokes field. Thus, the Stokes field can be assumed to be zero, and only the anti-Stokes field at frequency $\omega_c + \omega_m$ builds up in the cavity. The generated anti-Stokes field and the input probe field are degenerate, and the destructive interference happens between them, thus the absorption of the probe field goes to zero, resulting in the regular EIT for the probe field [3]. The second term in Eq. (10) is the contribution from the phonon-photon parametric process involving the mechanical drive acting on the waveguide. These two terms show that there are three pathways for the probe field passing through the system: (1) directly transmitting through the microdisk cavity, (2) interfering with the anti-Stokes field generated by scattering of the coupling field from the coherent mechanical oscillation induced by the radiation

pressure force and the reactive cavity optical force, and (3) interfering with the anti-Stokes field generated by scattering of the coupling field from the coherent mechanical oscillation induced directly by the mechanical drive. Thus, the output probe field is determined by the interference between these two terms or among these three pathways. If the system is in the unresolved-sideband regime, the Stokes field is not suppressed, thus the Stokes field cannot be assumed to be zero, and the output field contains the Stokes and anti-Stokes components.

We proceed by analyzing the output probe field normalized by the amplitude of the probe field $t_p(x) = \frac{\langle\delta\tilde{c}_{\text{out}}\rangle}{\varepsilon_p}$. It consists of two components,

$$t_p(x) = t_{p1}(x) + t_{p2}(x), \quad (11)$$

where $t_{p1}(x) = \mu\frac{J(x)}{d(x)} + \frac{g_\kappa c_s B_1(x)}{2\sqrt{\eta\kappa}(\frac{\gamma_m}{2} - ix)} - 1$, and $t_{p2}(x) = \left[\mu\frac{A}{d(x)} + \frac{g_\kappa c_s B_2(x)}{2\sqrt{\eta\kappa}(\frac{\gamma_m}{2} - ix)} \right] \frac{\varepsilon_d}{\varepsilon_p} e^{-i\phi}$. For convenience, the ratio of the amplitude of the mechanical drive to that of the probe field is defined as $\frac{\varepsilon_d}{\varepsilon_p} = u\sqrt{2\eta\kappa}$, where u is the amplitude parameter of the mechanical drive. In the absence of the coupling field and the mechanical drive ($g_\kappa = 0$ and $u = 0$), the output probe field $t_p(x)$ becomes

$$t_p(x) = \frac{2\eta\kappa}{\kappa - ix} - 1. \quad (12)$$

At the exact two-photon resonance $x = 0$, the output probe field is $t_p(0) = 2\eta - 1$, and the intensity of the output probe field is $|t_p(0)|^2 = |2\eta - 1|^2$. When the external and intrinsic decay rates of the cavity field are exactly equal ($\kappa_e = \kappa_i$), the microdisk cavity is critically coupled to the waveguide ($\eta = \frac{1}{2}$). In this case, the intensity $|t_p(0)|^2$ of the output probe field reaches its minimum value 0, thus the probe field is totally absorbed by the system.

It has been shown that the presence of the strong coupling field not only modifies the transmission of the weak probe field near resonance $x = 0$, but also leads to a very steep variation in the phase $\theta(x) = \arg[t_p(x)]$ of the output probe field near resonance $x = 0$, resulting in the group delay $\tau_g(x)$ of the output probe field [3–5]. The group delay of the output probe field can be calculated by

$$\tau_g(x) = \frac{\partial\theta(x)}{\partial x}. \quad (13)$$

The positive (negative) group delay of the output probe field corresponds to the slowing (advancing) of the output probe field.

We use the parameters from a recent experiment [15], which mainly discusses the reactive cavity optical force on the waveguide: the wavelength of the coupling field $\lambda = 1564.25$ nm, the mass of the waveguide $m = 2$ pg, the resonance frequency of the waveguide $\omega_m = 2\pi \times 25.45$ MHz, the damping rate of the waveguide $\gamma_m = \omega_m/5000$, and the total cavity decay rate $\kappa = 0.1\omega_m$, thus the system is well within the resolved-sideband regime ($\omega_m \gg \kappa$).

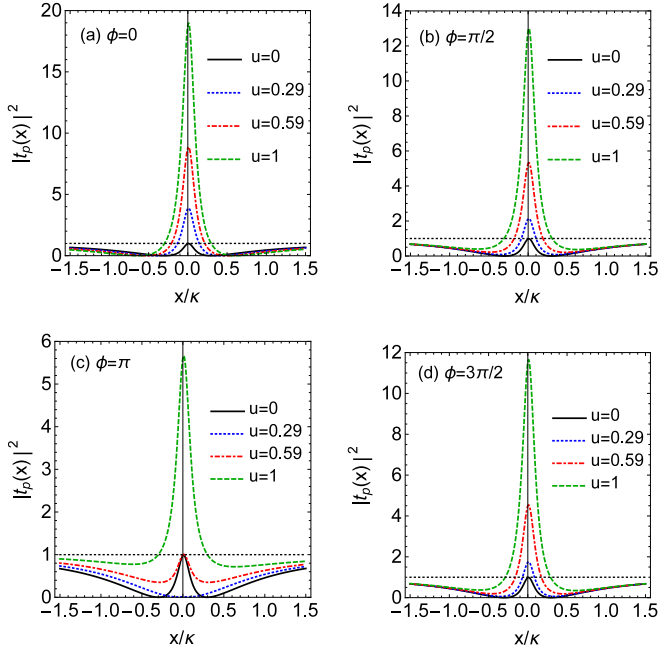


FIG. 2. The intensity $|t_p(x)|^2$ of the output probe field as a function of the normalized probe detuning x/κ for different values of the amplitude parameter u of the mechanical drive when $\eta = 0.5$, $\mathcal{G}_c = 10 \mu\text{W}$, and $\phi = 0, \pi/2, \pi, 3\pi/2$. (a) $\phi = 0$, (b) $\phi = \pi/2$, (c) $\phi = \pi$, (d) $\phi = 3\pi/2$. The black solid, blue dotted, red dot-dashed, and green dashed curves represent $u = 0, 0.29, 0.59$, and 1 , respectively. The flat dotted line represents $|t_p(x)|^2 = 1$.

III. THE INTENSITY OF THE OUTPUT PROBE FIELD IN THE PURELY DISSIPATIVE OPTOMECHANICAL SYSTEM

In this section, we show how the amplitude parameter u and phase ϕ of the weak mechanical drive and the power \mathcal{G}_c of the coupling field affect the intensity $|t_p(x)|^2$ of the output probe field in the purely dissipative optomechanical system in both the critical coupling regime and the undercoupling regime. The dissipative optomechanical coupling strength is chosen to be $g_\kappa = -2\pi \times 26.6 \text{ MHz/nm} \times q_{zpf}$ [15].

A. Perfect absorption, EIT-like effect, amplification for the probe field in the critical coupling regime

It is noted that the critical coupling ($\eta = 0.5$) between the microdisk cavity and the waveguide is achievable in the experiment [15]. When the system is in the critical coupling regime, and the power of the coupling field is $\mathcal{G}_c = 10 \mu\text{W}$, the steady-state displacement q_s of the waveguide is found to be about $-3.37 \times 10^{-13} \text{ m}$, which is very small, thus the approximation of $\kappa_e(q)$ in Eq. (2) is reasonable. Figure 2 plots the intensity $|t_p(x)|^2$ of the output probe field against the normalized probe detuning x/κ for different values of the amplitude parameter u of the mechanical drive when $\eta = 0.5$, $\mathcal{G}_c = 10 \mu\text{W}$, and $\phi = 0, \pi/2, \pi, 3\pi/2$. Without the mechanical drive ($u = 0$) (Fig. 2), the intensity $|t_p(x)|^2$ exhibits a transparency peak at $x = 0$, and the peak value $|t_p(0)|^2$ is approximately equal to unity, which is when the EIT effect occurs [18,33]; thus, the input probe field is almost totally transmitted through the system, and the absorption of the

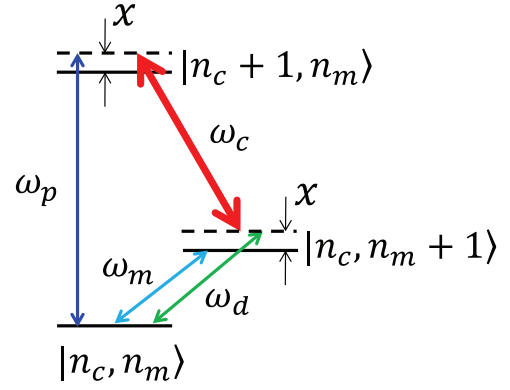


FIG. 3. Energy-level diagram for the optomechanical system. The transition $|n_c, n_m\rangle \rightarrow |n_c + 1, n_m\rangle$ is the cavity excitation (photon) at frequency ω_c , and the transition $|n_c, n_m\rangle \rightarrow |n_c, n_m + 1\rangle$ is the mechanical excitation (phonon) at frequency ω_m , where n_c and n_m denote the intracavity photon number and the phonon number in the waveguide, respectively. The coupling field with frequency ω_c drives the transition $|n_c, n_m + 1\rangle \leftrightarrow |n_c + 1, n_m\rangle$, the probe field with frequency ω_p and detuning x probes the transition $|n_c, n_m\rangle \leftrightarrow |n_c + 1, n_m\rangle$, and the mechanical pump with frequency ω_d and detuning x drives the transition $|n_c, n_m\rangle \leftrightarrow |n_c, n_m + 1\rangle$.

probe field by the system is almost zero. From the energy-level diagram for the system as shown in Fig. 3, the zero absorption of the probe field can be understood as a result of the destructive interference between the input probe field at frequency ω_p and the anti-Stokes field at frequency $\omega_c + \omega_m$ generated by the interaction of the coupling field with the mechanical phonons driven by the reactive cavity optical force. Our calculations show that the coupling power \mathcal{G}_c required to observe the EIT must be less than the critical power $\mathcal{G}_{cr} = \frac{\kappa(\kappa - \frac{\gamma_m}{2})^2}{2g_\kappa^2} \hbar\omega_c \simeq 28.15 \mu\text{W}$. The linewidth of the transparency peak can be estimated by $\frac{\gamma_m}{2} + \frac{g_\kappa^2 \epsilon_c^2}{2\kappa^2}$. Thus, the transparency peak becomes wider with an increase in the coupling power \mathcal{G}_c [18,33]. If the coupling power \mathcal{G}_c is larger than the critical power \mathcal{G}_{cr} , the system enters the strong coupling regime, and normal mode splitting occurs [32,33]. With the mechanical drive ($u \neq 0$), for $\phi = 0, \pi/2$, and $3\pi/2$ [Figs. 2(a), 2(b), and 2(d)], it is seen that the intensity $|t_p(0)|^2$ is larger than unity and increases with increasing the value of u , thus the probe field is amplified and becomes larger for a larger value of u . This result is also seen in Fig. 4, which plots the intensity $|t_p(0)|^2$ of the output probe field against the amplitude parameter u of the mechanical drive for different phases ϕ of the mechanical drive when $\eta = 0.5$ and $\mathcal{G}_c = 10 \mu\text{W}$. It is noted that the electromagnetically induced amplification can be obtained in a dispersive optomechanical system driven by a blue-detuned coupling field [4,6,11]. However, for $\phi = \pi$ [Fig. 2(c)], with increasing the amplitude parameter u , the intensity $|t_p(0)|^2$ first decreases and then increases. This trend is also seen in Fig. 4. A similar result is obtained in the dispersive case [35]. When $u = 0.29$, the intensity $|t_p(0)|^2$ takes its minimum value about 0.01, thus the probe field is almost totally absorbed by the system. This is due to the constructive interference among the input probe field at frequency ω_p , the anti-Stokes field at frequency $\omega_c + \omega_m$ produced by the interaction of the coupling field with the mechanical phonons induced by the

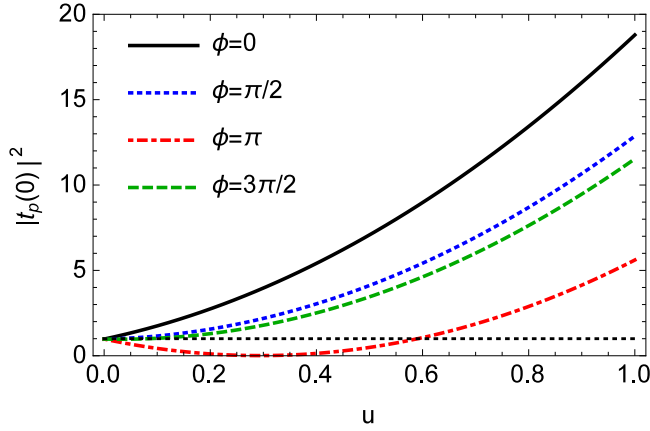


FIG. 4. The intensity $|t_p(0)|^2$ of the output probe field as a function of the amplitude parameter u of the mechanical drive for different phases ϕ of the mechanical drive when $\eta = 0.5$ and $\varrho_c = 10 \mu\text{W}$. The black solid, blue dotted, red dot-dashed, and green dashed curves represent $\phi = 0, \pi/2, \pi$, and $3\pi/2$, respectively. The flat dotted line represents $|t_p(0)|^2 = 1$.

reactive cavity optical force, and the anti-Stokes field at frequency $\omega_c + \omega_m$ produced by the interaction of the coupling field with the mechanical phonons induced directly by the mechanical drive, which can be seen from the energy-level diagram for the system as shown in Fig. 3. Note that the nearly perfect absorption of the probe field is also the result of the almost complete destructive interference between the two terms in Eq. (11). It is worth mentioning that a similar perfect absorption occurs in a dispersive optomechanical system with two weak counterpropagating probe fields [39]. In Fig. 2(c), when $u = 0.59$, the intensity $|t_p(x)|^2$ exhibits the EIT-like transparency peak with $|t_p(0)|^2 \simeq 1$, thus one observes the nearly full transmission of the probe field at $x = 0$, and there is almost no absorption of the probe field, which is the result of the destructive interference among the input probe field at frequency ω_p and the two anti-Stokes fields at the same frequency $\omega_c + \omega_m$ as mentioned before. Furthermore, when $u > 0.59$, the intensity $|t_p(0)|^2$ is larger than unity, which indicates the amplification of the probe field. Therefore, in the critical coupling regime, the system can switch from the EIT to the nearly full absorption, to the EIT-like behavior, and then to the amplification of the probe field by gradually increasing the amplitude parameter u of the mechanical drive with the phase $\phi = \pi$. Figure 5 shows the intensity $|t_p(0)|^2$ of the output probe field against the coupling power ϱ_c for different values of the amplitude parameter u of the mechanical drive when $\eta = 0.5$ and $\phi = 0, \pi$. In order to ensure the validity of the linearized equations (7), the mechanical displacement fluctuation $\langle \delta Q \rangle$ defined by $\langle \delta Q \rangle = \frac{1}{\sqrt{2}}(\langle \delta \tilde{b} \rangle + \langle \delta \tilde{b}^\dagger \rangle)$ must be much less than the steady-state mechanical displacement Q_s . Figure 6 shows the ratio $|\langle \delta Q \rangle / Q_s|$ at the two-photon resonance $x = 0$ as a function of the power ϱ_c of the coupling field for different values of the amplitude parameter u of the mechanical drive when $\eta = 0.5$ and $\phi = 0, \pi$. In Fig. 6(a), for $u = 0, 0.29, 0.59$, and 1 , and $\phi = 0$, we find that $|\langle \delta Q \rangle / Q_s|$ is always less than 0.076 as the coupling power ϱ_c increases from $0.5 \mu\text{W}$ to $28 \mu\text{W}$. In Fig. 6(b), for $u = 0, 0.29, 0.59$, and 1 , and $\phi = \pi$, we find that $|\langle \delta Q \rangle / Q_s|$ is

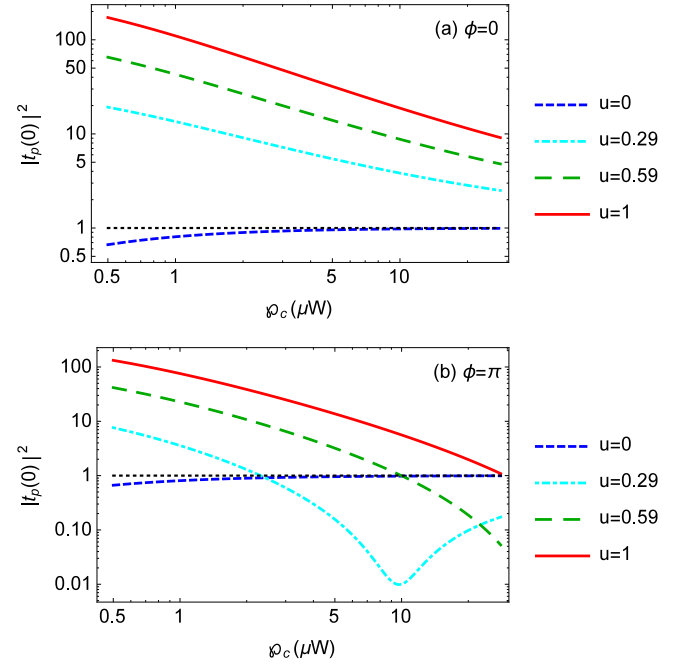


FIG. 5. The intensity $|t_p(0)|^2$ of the output probe field as a function of the power ϱ_c of the coupling field for different values of the amplitude parameter u of the mechanical drive when $\eta = 0.5$ and $\phi = 0, \pi$. (a) $\phi = 0$ and (b) $\phi = \pi$. The blue short-dashed, cyan dot-dashed, green long-dashed, and red solid curves represent $u = 0, 0.29, 0.59$, and 1 , respectively. The flat dotted line represents $|t_p(0)|^2 = 1$.

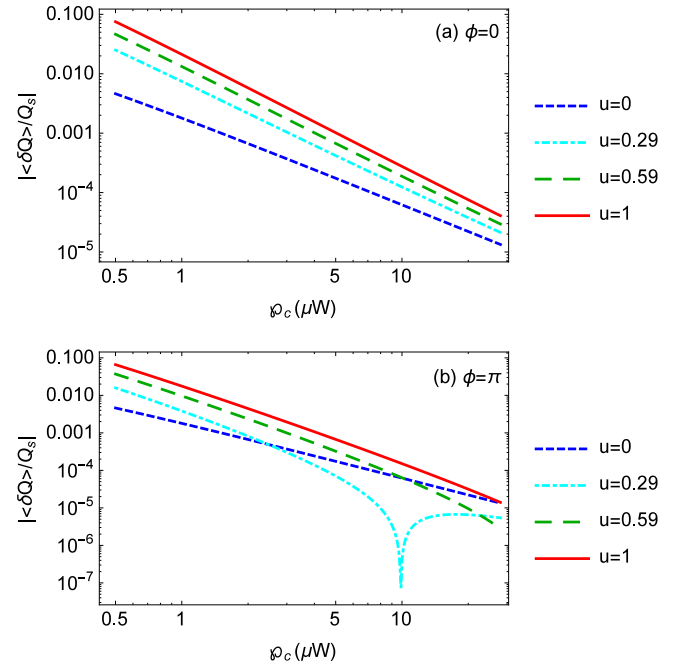


FIG. 6. The ratio $|\langle \delta Q \rangle / Q_s|$ at $x = 0$ as a function of the power ϱ_c of the coupling field for different values of the amplitude parameter u of the mechanical drive when $\eta = 0.5$ and $\phi = 0, \pi$. (a) $\phi = 0$ and (b) $\phi = \pi$. The blue short-dashed, cyan dot-dashed, green long-dashed, and red solid curves represent $u = 0, 0.29, 0.59$, and 1 , respectively.

always less than 0.066 as the coupling power g_{λ} increases from $0.5 \mu\text{W}$ to $28 \mu\text{W}$. Thus, for $u = 0, 0.29, 0.59$, and 1 , and $\phi = 0, \pi$, the condition $|\langle \delta Q \rangle / Q_s| \ll 1$ can be satisfied when the coupling power g_{λ} is not less than $0.5 \mu\text{W}$. Now, we look at the intensity $|t_p(0)|^2$ of the output probe field for $\phi = 0$, as shown in Fig. 5(a). In the absence of the mechanical drive ($u = 0$), with increasing the coupling power g_{λ} from $0.5 \mu\text{W}$ to $28 \mu\text{W}$, the intensity $|t_p(0)|^2$ increases, and finally saturates at unity, thus the system displays the EIT effect. Using Eq. (11), we find that the output probe field $t_p(0)$ for $u = 0$ is $t_p(0) \simeq 1 - \frac{\kappa \frac{\gamma_m}{2}}{(\frac{g_{\lambda}}{\sqrt{2\kappa}} \varepsilon_c)^2 + \kappa \frac{\gamma_m}{2}}$, thus the output probe intensity $|t_p(0)|^2$ increases with an increase in the coupling power g_{λ} , which is consistent with the numerical result in Fig. 5(a). It is found that we can approach complete transmission $[|t_p(0)|^2 = 1]$ in the limit of the strong coupling field $(\frac{g_{\lambda}}{\sqrt{2\kappa}} \varepsilon_c)^2 \gg \kappa \frac{\gamma_m}{2}$, which is equivalent to $g_{\lambda} \gg \frac{\kappa^2 \gamma_m}{g_s^2} \hbar \omega_c \simeq 113 \text{ nW}$. In the presence of the mechanical drive ($u \neq 0$), as the coupling power g_{λ} increases from $0.5 \mu\text{W}$ to $28 \mu\text{W}$, the intensity $|t_p(0)|^2$ decreases, and is always larger than unity, thus the probe field is amplified. For $u = 0.29, 0.59$, and 1 , the intensity $|t_p(0)|^2$ takes its maximum value about 19.2, 65.3, and 172.4 at $g_{\lambda} = 0.5 \mu\text{W}$, respectively. Hence, for a larger value of u , the maximum intensity $|t_p(0)|^2$ is larger. Therefore, it is possible to dramatically amplify a weak probe field by applying a mechanical drive with the phase $\phi = 0$ to the waveguide in the critical coupling regime. Physically, the amplification of the probe field is due to the contribution of the phonon-photon parametric process involving the mechanical drive described by the second term in Eq. (11), which depends on the amplitude parameter u of the mechanical drive and the power g_{λ} of the coupling field. On one hand, a larger amplitude parameter u of the mechanical drive can excite more phonons in the waveguide, which leads to a stronger anti-Stokes field at frequency $\omega_c + \omega_m$. On the other hand, a larger coupling power g_{λ} can generate more photons in the cavity but reduce the phonon number in the waveguide since the dissipative optomechanical coupling induces the cooling of the waveguide in the resolved-sideband limit, which leads to a weaker anti-Stokes field at frequency $\omega_c + \omega_m$. Thus, a maximal amplification of the probe field exists as a result of the competition between these two processes.

Next, we look at the case of $\phi = \pi$, as shown in Fig. 5(b). For comparison, we also plot the intensity $|t_p(0)|^2$ in the absence of the mechanical drive ($u = 0$) in Fig. 5(b). In the presence of the mechanical drive ($u \neq 0$), according to Eq. (11), complete transmission $[|t_p(0)|^2 = 1]$ occurs at the coupling power $g_{\lambda} \simeq \frac{\kappa^3 \hbar \omega_c}{8g_s^2} (u + \sqrt{u^2 - 4\frac{\gamma_m}{\kappa}})^2$, which shows that complete transmission appears at a larger coupling power g_{λ} for a larger value of u . For $u = 0.29, 0.59$, and 1 , g_{λ} is about 2.26, 10.00, and 28.09 μW , respectively. In addition, from Fig. 5(b), for $u = 0.29, 0.59$, and 1 , when the coupling power g_{λ} is larger than $0.5 \mu\text{W}$ but less than g_{λ} , the intensity $|t_p(0)|^2$ is larger than unity, thus the incident probe field is amplified. Hence, for a larger value of u , the probe field can be amplified over a wider range of the coupling power g_{λ} . For $u = 0.29, 0.59$, and 1 , the intensity $|t_p(0)|^2$ takes its maximum value about 7.6, 41.7, and 132.4 at $g_{\lambda} = 0.5 \mu\text{W}$, respectively. Hence, for a larger value of u , the maximum intensity $|t_p(0)|^2$ is larger. For a given value of u , it is noted that the

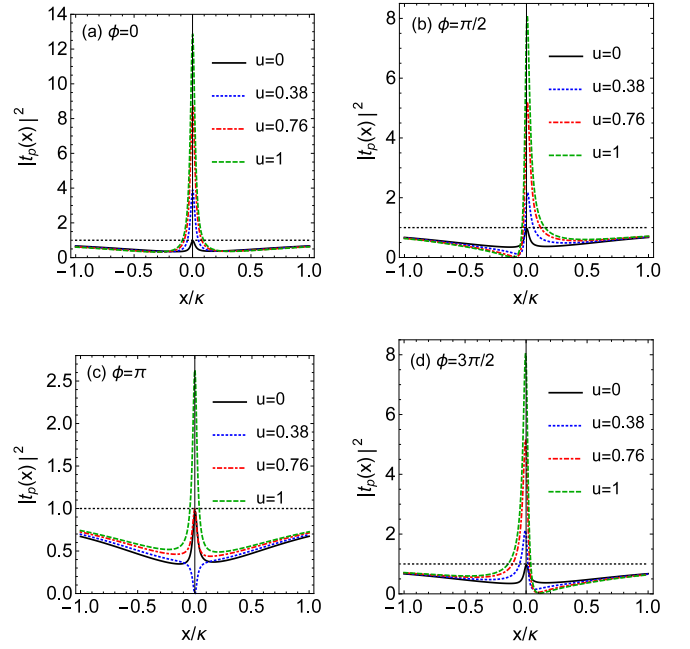


FIG. 7. The intensity $|t_p(x)|^2$ of the output probe field as a function of the normalized probe detuning x/κ for different values of the amplitude parameter u of the mechanical drive when $\eta = 0.2$, $g_{\lambda} = 1 \mu\text{W}$, and $\phi = 0, \pi/2, \pi, 3\pi/2$. (a) $\phi = 0$, (b) $\phi = \pi/2$, (c) $\phi = \pi$, (d) $\phi = 3\pi/2$. The black solid, blue dotted, red dot-dashed, and green dashed curves represent $u = 0, 0.38, 0.76$, and 1 , respectively. The flat dotted line represents $|t_p(x)|^2 = 1$.

maximum intensity $|t_p(0)|^2$ for $\phi = \pi$ is less than that for $\phi = 0$. Furthermore, from Eq. (11), it is found that perfect absorption $|t_p(0)|^2 = 0$ occurs at the coupling power $g_{\lambda} \simeq \frac{2u^2 \kappa^3}{g_s^2} \hbar \omega_c$, which indicates that perfect absorption happens at a larger coupling power g_{λ} for a larger value of u . For $u = 0.29, 0.59$, and 1 , nearly perfect absorption $[|t_p(0)|^2 \simeq 0.01]$ happens at $g_{\lambda} \simeq 10.0, 39.3$, and $112.8 \mu\text{W}$, respectively. Thus, only when $u = 0.29$, nearly perfect absorption occurs within the range of the coupling power g_{λ} from $0.5 \mu\text{W}$ to $28 \mu\text{W}$, as shown in Fig. 5(b). The above results demonstrate the possibility to achieve the amplification, full transmission, and nearly perfect absorption of the probe field by changing the coupling power g_{λ} when the mechanical drive with the phase $\phi = \pi$ is applied to the waveguide in the critical coupling regime.

B. EIA-like effect, EIT-like effect, amplification for the probe field in the undercoupling regime

When the system is in the undercoupling regime ($\eta = 0.2$), and the power of the coupling field is $g_{\lambda} = 1 \mu\text{W}$, the steady-state displacement q_s of the waveguide is found to be about $-3.36 \times 10^{-14} \text{ m}$, which is very small, thus the approximation of $\kappa_e(q)$ in Eq. (2) holds.

Figure 7 plots the intensity $|t_p(x)|^2$ of the output probe field against the normalized probe detuning x/κ for different values of the amplitude parameter u of the mechanical drive when $\eta = 0.2$, $g_{\lambda} = 1 \mu\text{W}$, and $\phi = 0, \pi/2, \pi, 3\pi/2$. When the mechanical drive is absent ($u = 0$) (Fig. 7), the intensity $|t_p(x)|^2$ has a transparency peak at $x = 0$, and $|t_p(0)|^2 \simeq 1$,

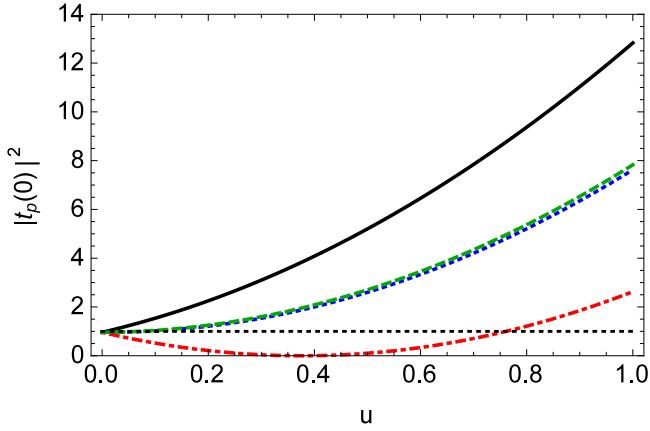


FIG. 8. The intensity $|t_p(0)|^2$ of the output probe field as a function of the amplitude parameter u of the mechanical drive for different phases ϕ of the mechanical drive when $\eta = 0.2$ and $\mathcal{E}_c = 1 \mu\text{W}$. The black solid, blue dotted, red dot-dashed, and green dashed curves represent $\phi = 0, \pi/2, \pi,$ and $3\pi/2$, respectively. The flat dotted line represents $|t_p(0)|^2 = 1$.

thus the EIT effect happens. To induce the EIT effect, the coupling power \mathcal{E}_c must be less than the critical power $\mathcal{E}_{cr} = \frac{\eta\kappa(\kappa - \frac{\gamma_m}{2})^2 \hbar\omega_c}{g_k^2} \simeq 11.26 \mu\text{W}$. The linewidth of the transparency peak can be estimated by $\frac{\gamma_m}{2} + \frac{g_k^2 \epsilon_c^2}{4\eta\kappa^2}$. Next, we see the case with the mechanical drive ($u \neq 0$). For $\phi = 0, \pi$ [Figs. 7(a) and 7(c)], it is seen that the intensity $|t_p(x)|^2$ is almost symmetric about $x = 0$, respectively. For $\phi = \pi/2, 3\pi/2$ [Figs. 7(b) and 7(d)], it is seen that the intensity $|t_p(x)|^2$ is asymmetric about $x = 0$, respectively, and they are almost mirror images of each other. These results are similar to those in the dispersive case [34]. For $\phi = 0, \pi/2,$ and $3\pi/2$ [Figs. 7(a), 7(b), and 7(d)], the intensity $|t_p(0)|^2$ is larger than unity and increases as the value of u increases, thus the probe field is amplified and becomes larger as the value of u increases. This result is also seen in Fig. 8, which plots the intensity $|t_p(0)|^2$ of the output probe field against the amplitude parameter u of the mechanical drive for different phases ϕ of the mechanical drive when $\eta = 0.2$ and $\mathcal{E}_c = 1 \mu\text{W}$. However, for $\phi = \pi$ [Fig. 7(c)], with increasing the amplitude parameter u , the intensity $|t_p(0)|^2$ first reduces and then increases. This trend is also seen in Fig. 8. In Fig. 7(c), when $u = 0.38$, the intensity $|t_p(x)|^2$ exhibits the EIA-like feature with a very narrow dip at $x = 0$, and $|t_p(0)|^2 \simeq 0$, thus the probe field is almost totally absorbed by the system. It is worth mentioning that the EIA can be obtained in a dispersive optomechanical system [4,11] and a dissipative optomechanical system [18] in the presence of a blue-detuned coupling field. In addition, the EIA can be realized in a double-cavity dispersive optomechanical system, in which the two cavity fields are respectively driven by a red-detuned coupling field and an absorption peak appears in a transparent window [12]. In Fig. 7(c), when $u = 0.76$, the intensity $|t_p(x)|^2$ exhibits the EIT-like feature with $|t_p(0)|^2 \simeq 1$, thus the probe field almost totally passes through the system at $x = 0$. When $u > 0.76$, the intensity $|t_p(0)|^2$ is larger than unity, thus the probe field is amplified. Hence, in the undercoupling regime, the system can switch from EIT to EIA-like behavior, to EIT-like

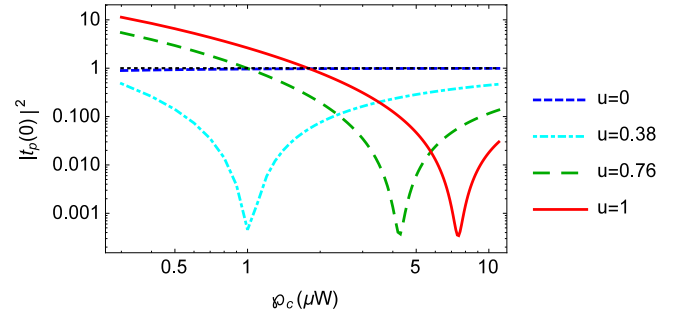


FIG. 9. The intensity $|t_p(0)|^2$ of the output probe field as a function of the power \mathcal{E}_c of the coupling field for different values of the amplitude parameter u of the mechanical drive when $\eta = 0.2$ and $\phi = \pi$. The blue short-dashed, cyan dot-dashed, green long-dashed, and red solid curves represent $u = 0, 0.38, 0.76,$ and 1 , respectively. The flat dotted line represents $|t_p(0)|^2 = 1$.

behavior, and then to amplification of the probe field by gradually increasing the amplitude parameter u of the mechanical drive with the phase $\phi = \pi$.

Figures 9 and 10 show the intensity $|t_p(0)|^2$ of the output probe field and the ratio $|\langle \delta Q \rangle / Q_s|$ at $x = 0$ against the power \mathcal{E}_c of the coupling field for different values of the amplitude parameter u of the mechanical drive when $\eta = 0.2$ and $\phi = \pi$. In Fig. 10, for $u = 0, 0.38, 0.76,$ and 1 , we find that $|\langle \delta Q \rangle / Q_s|$ is always less than 0.049 as the coupling power \mathcal{E}_c increases from 0.3 μW to 11 μW . Thus, for $u = 0, 0.38, 0.76,$ and 1 , the condition $|\langle \delta Q \rangle / Q_s| \ll 1$ can be satisfied when the coupling power \mathcal{E}_c is not less than 0.3 μW . In Fig. 9, without the mechanical drive ($u = 0$), as the coupling power \mathcal{E}_c increases from 0.3 μW to 11 μW , the intensity $|t_p(0)|^2$ increases, and finally saturates at unity, thus the EIT effect occurs. Using Eq. (11), we find $t_p(0) \simeq 1 - \frac{\kappa\gamma_m\eta}{(\frac{g_k}{2\sqrt{\eta\kappa}}\epsilon_c)^2 + \kappa\frac{\gamma_m}{2}}$, thus the output probe intensity $|t_p(0)|^2$ increases with increasing the coupling power \mathcal{E}_c , which is in agreement with the numerical result in Fig. 9. It is noted that complete transmission ($|t_p(0)|^2 = 1$) can be approached in the limit of the strong coupling field

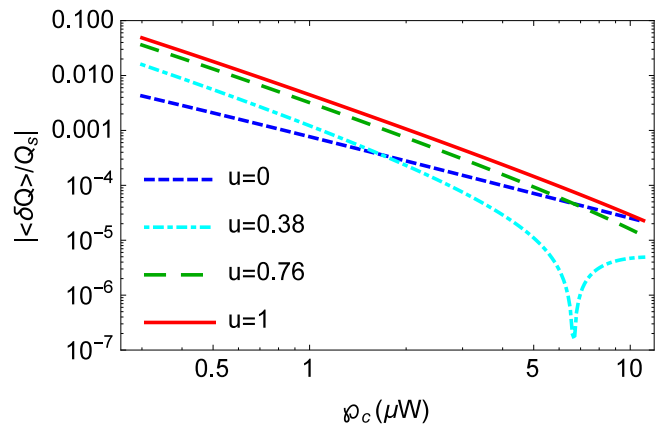


FIG. 10. The ratio $|\langle \delta Q \rangle / Q_s|$ at $x = 0$ as a function of the power \mathcal{E}_c of the coupling field for different values of the amplitude parameter u of the mechanical drive when $\eta = 0.2$ and $\phi = \pi$. The blue short-dashed, cyan dot-dashed, green long-dashed, and red solid curves represent $u = 0, 0.38, 0.76,$ and 1 , respectively.

$(\frac{g_\kappa}{2\sqrt{\eta\kappa}}\varepsilon_c)^2 \gg \kappa\frac{\gamma_m}{2}$, which is equivalent to $g_\kappa \gg \frac{2\eta\kappa^2\gamma_m}{g_\kappa^2}\hbar\omega_c \simeq 45.2$ nW. With the mechanical drive ($u \neq 0$), as the coupling power g_κ increases from 0.3 μ W to 11 μ W, the intensity $|t_p(0)|^2$ first decreases and then increases. From Eq. (11), it is found that perfect absorption [$|t_p(0)|^2 = 0$] occurs at the coupling power $g_\kappa \simeq \frac{4\eta^3\kappa^3\hbar\omega_c}{g_\kappa^2}[u + \sqrt{u^2 - \frac{\gamma_m}{2\kappa\eta^2}(1-2\eta)}]^2$, which increases with an increase in the amplitude parameter u . For $u = 0.38, 0.76$, and 1 , nearly perfect absorption [$|t_p(0)|^2 < 0.001$] occurs at $g_\kappa \simeq 1.0, 4.2$, and 7.5 μ W, respectively. Moreover, from Eq. (11), it is found that complete transmission [$|t_p(0)|^2 = 1$] appears at the coupling power $g_\kappa' \simeq \frac{\eta^3\kappa^3\hbar\omega_c}{g_\kappa^2}[u + \sqrt{u^2 - 2\frac{\gamma_m}{\kappa\eta^2}(1-\eta)}]^2$, which becomes larger with increasing the amplitude parameter u . For $u = 0.76, 1$, complete transmission happens at $g_\kappa' \simeq 1.0$ and 1.8 μ W, respectively. In addition, for $u = 0.76, 1$, when the coupling power g_κ is larger than 0.3 μ W but less than g_κ' , the intensity $|t_p(0)|^2$ is larger than unity, thus the incident probe field is amplified. For $u = 0.38, 0.76$, and 1 , the intensity $|t_p(0)|^2$ takes its maximum value about $0.5, 5.4$, and 11.3 at $g_\kappa = 0.3$ μ W, respectively. Thus, increasing the value of u makes the maximum intensity $|t_p(0)|^2$ larger, which is the same as that for $\phi = \pi$ in the critical coupling regime. For $u = 1$, it is seen that the maximum intensity $|t_p(0)|^2$ is smaller than that for $\phi = \pi$ in the critical coupling regime. Therefore, when a mechanical drive with the phase $\phi = \pi$ is applied to the waveguide in the undercoupling regime, it is possible to achieve nearly perfect absorption, complete transmission, and amplification of the probe field by adjusting the coupling power g_κ .

In Ref. [34], Jia *et al.* have discussed the propagation of a weak probe field through a dispersive optomechanical system with an additional mechanical drive in both the undercoupling regime ($\kappa_e = 0.05\kappa$) and the overcoupling regime ($\kappa_e = \kappa$). They have shown that EIA-like behavior can be turned into EIT-like behavior in the undercoupling regime if the total phase of the coupling, probe, and mechanical fields is changed from 0 to π . And, they have found that the maximum intensities of the output probe field appear approximately at the same coupling power for different amplitudes of the mechanical drive in the overcoupling regime ($\kappa_e = \kappa$). In contrast, in this present work, we have shown the propagation of a weak probe field through a dissipative optomechanical system with an additional mechanical drive in both the critical coupling regime ($\kappa_e = 0.5\kappa$) and the undercoupling regime ($\kappa_e = 0.2\kappa$). We find that the maximum intensities of the output probe field occur at the same coupling powers for different amplitudes of the mechanical drive in both the critical coupling regime and the undercoupling regime. Under the action of the mechanical drive with the phase $\phi = \pi$, we show that it is possible to convert EIA-like behavior to EIT-like behavior in the undercoupling regime by increasing the amplitude of the mechanical drive.

IV. THE GROUP DELAY OF THE OUTPUT PROBE FIELD IN THE PURELY DISSIPATIVE OPTOMECHANICAL SYSTEM

In this section, we show the influence of the amplitude parameter u and phase ϕ of the mechanical drive on the

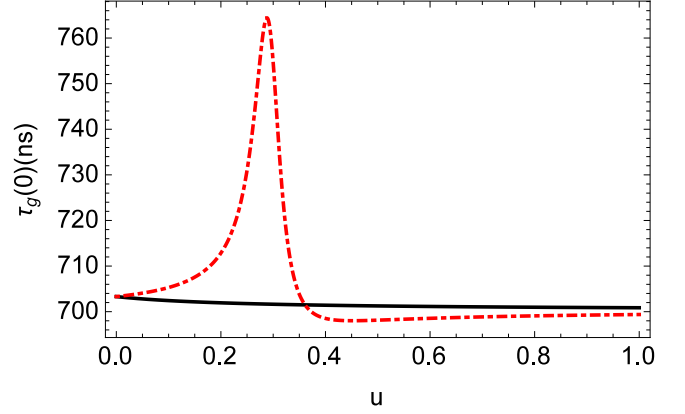


FIG. 11. The group delay $\tau_g(0)$ of the output probe field as a function of the amplitude parameter u of the mechanical drive when $\eta = 0.5$, $g_\kappa = 10$ μ W, and $\phi = 0, \pi$. The black solid and red dot-dashed curves represent $\phi = 0$ and $\phi = \pi$, respectively.

group delay $\tau_g(x)$ of the output probe field at resonance $x = 0$ in the purely dissipative optomechanical system in both the critical coupling regime and the undercoupling regime. It is noted that the phase $\theta(x)$ of the output probe field is given by $\theta(x) = \frac{1}{2i} \ln \frac{t_p(x)}{t_p^*(x)}$. Thus, from Eq. (13), it is found that the group delay $\tau_g(x)$ of the output probe field can be calculated by $\tau_g(x) = \text{Im}[\frac{1}{t_p(x)} \frac{\partial t_p(x)}{\partial x}]$. The dissipative optomechanical coupling strength is still chosen to be $g_\kappa = -2\pi \times 26.6$ MHz/nm $\times q_{zpf}$ [15]. Figure 11 shows the dependence of the group delay $\tau_g(0)$ of the output probe field on the amplitude parameter u of the mechanical drive when $\eta = 0.5$, $g_\kappa = 10$ μ W, and $\phi = 0, \pi$. When $\phi = 0$, with increasing the amplitude parameter u from 0 to 1 , the group delay $\tau_g(0)$ decreases from 703 ns to 701 ns, thus the amplitude parameter u has little effect on the group delay $\tau_g(0)$ of the output probe field. Next, we look at the case of $\phi = \pi$. As the amplitude parameter u increases from 0 to 0.29 , the group delay $\tau_g(0)$ increases, and it reaches its maximum value about 764 ns (corresponding to about 3.89π times the cavity photon lifetime κ^{-1}) at $u = 0.29$, at which the nearly perfect absorption occurs as shown in Fig. 2(c). As the amplitude parameter u increases further from 0.29 to 0.45 , the group delay $\tau_g(0)$ decreases, and it reaches its minimum value about 698 ns (corresponding to about 3.55π times the cavity photon lifetime κ^{-1}) at $u = 0.45$. As the amplitude parameter u increases further from 0.45 to 1 , the group delay $\tau_g(0)$ increases a little to about 699 ns. Therefore, in the critical coupling regime, compared to the case of $\phi = 0$, we find that the positive group delay $\tau_g(0)$ of the output probe field can be largely increased by changing the amplitude parameter u of the mechanical drive with the phase $\phi = \pi$, which implies that the output probe field can be slowed down largely. Figure 12 shows the dependence of the group delay $\tau_g(0)$ of the output probe field on the amplitude parameter u of the mechanical drive when $\eta = 0.2$, $g_\kappa = 1$ μ W, and $\phi = 0, \pi$. When $\phi = 0$, with increasing the amplitude parameter u from 0 to 1 , the group delay $\tau_g(0)$ increases from 1.0 μ s to 2.2 μ s, thus the amplitude parameter u slightly affects the group delay $\tau_g(0)$ of the output probe field. Next, we consider the case of $\phi = \pi$. As the amplitude parameter u increases from 0 to 1 ,

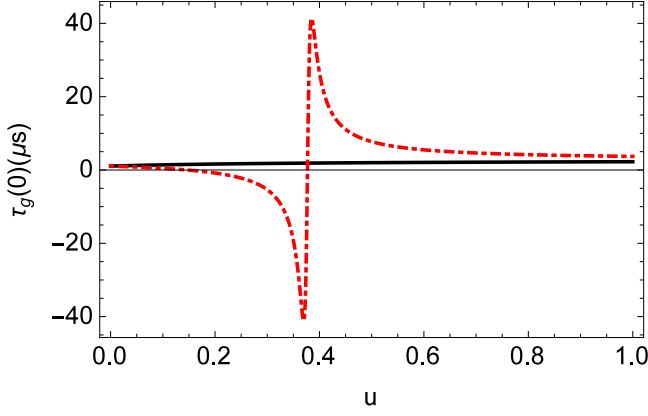


FIG. 12. The group delay $\tau_g(0)$ of the output probe field as a function of the amplitude parameter u of the mechanical drive when $\eta = 0.2$, $\mathcal{E}_c = 1 \mu\text{W}$, and $\phi = 0, \pi$. The black solid and red dot-dashed curves represent $\phi = 0$ and $\phi = \pi$, respectively.

the group delay $\tau_g(0)$ decreases from a positive value ($1.0 \mu\text{s}$) to a large negative value ($-41.1 \mu\text{s}$, corresponding to about -209.2π times the cavity photon lifetime κ^{-1}), then increases sharply to a large positive value ($41.4 \mu\text{s}$, corresponding to about 210.7π times the cavity photon lifetime κ^{-1}), and then decreases again to a positive value ($3.7 \mu\text{s}$). The group delay $\tau_g(0)$ takes its minimum value $-41.1 \mu\text{s}$ at $u = 0.37$, and takes its maximum value $41.4 \mu\text{s}$ at $u = 0.385$. Thus, the group delay $\tau_g(0)$ changes dramatically around $u = 0.38$, at which the EIA-like effect appears, as shown in Fig. 7(c). A similar result is obtained in the dispersive case [35]. Therefore, in the undercoupling regime, by adjusting the amplitude parameter u of the mechanical drive with the phase $\phi = \pi$, the group delay of the output probe field can be switched from a large negative value to a large positive value and vice versa, thus the slowing and advancing of the output probe field is switchable, which differs from the case of $\phi = 0$.

V. THE OPTICAL RESPONSE OF THE OPTOMECHANICAL SYSTEM WITH COMBINED DISPERSIVE AND DISSIPATIVE COUPLING

In the previous sections, we have considered the optical response of a purely dissipative optomechanical system with an additional weak mechanical drive for simplicity. In this section, we show the effect of the amplitude parameter u and phase ϕ of the weak mechanical drive on the optical response of an optomechanical system with combined dispersive and dissipative coupling. The dissipative and dispersive optomechanical coupling strengths are chosen to be $g_\kappa = -2\pi \times 26.6 \text{ MHz/nm} \times q_{z\text{pf}}$ and $g_\omega = 2\pi \times 2 \text{ MHz/nm} \times q_{z\text{pf}}$ [15], respectively. It is noted that the dispersive optomechanical coupling is much weaker than the dissipative optomechanical coupling. In the critical coupling regime ($\eta = 0.5$), when the power of the coupling field is $\mathcal{E}_c = 10 \mu\text{W}$, the steady-state mechanical displacement q_s is found to be about $-3.38 \times 10^{-13} \text{ m}$, which is very small, thus the approximations of $\omega_0(q)$ and $\kappa_c(q)$ in Eq. (2) hold. Figure 13 shows the intensity $|t_p(0)|^2$ and group delay $\tau_g(0)$ of the output probe field against the amplitude parameter u of the mechanical drive

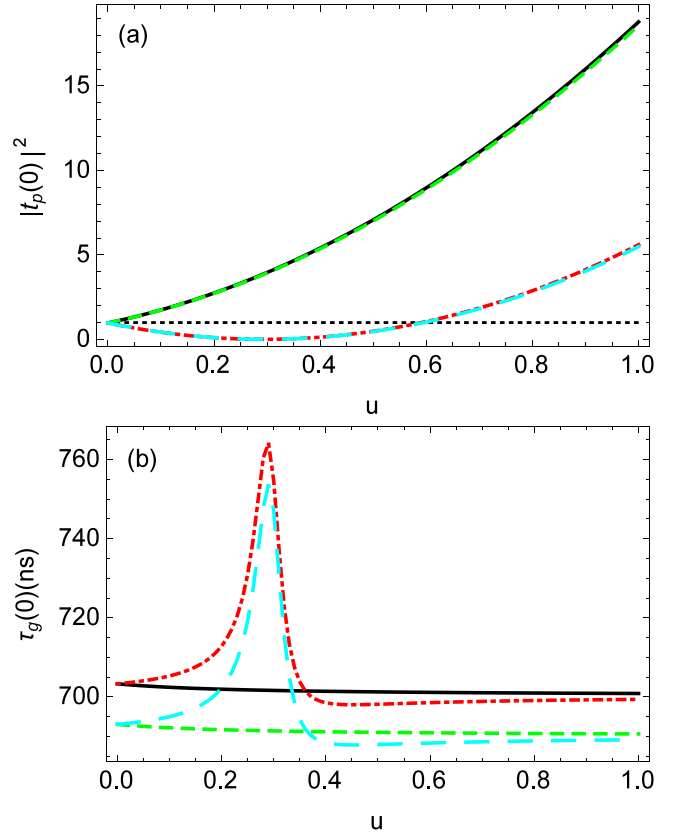


FIG. 13. The (a) intensity $|t_p(0)|^2$ and (b) group delay $\tau_g(0)$ of the output probe field as a function of the amplitude parameter u of the mechanical drive when $\eta = 0.5$, $\mathcal{E}_c = 10 \mu\text{W}$, and $\phi = 0, \pi$. The green short-dashed and cyan long-dashed curves correspond to the case of the combined dissipative and dispersive coupling, and they represent $\phi = 0$ and $\phi = \pi$, respectively. The black solid and red dot-dashed curves correspond to the case of purely dissipative coupling, and they represent $\phi = 0$ and $\phi = \pi$, respectively. The flat dotted line in (a) represents $|t_p(0)|^2 = 1$.

when $\eta = 0.5$, $\mathcal{E}_c = 10 \mu\text{W}$, and $\phi = 0, \pi$. In Fig. 13(a), for $\phi = 0, \pi$, it is seen that the intensities $|t_p(0)|^2$ in the case of the combined dispersive and dissipative coupling are almost equal to those in the purely dissipative coupling case, respectively. In Fig. 13(b), for $\phi = 0$, it is seen that the group delay $\tau_g(0)$ in the case of the combined dispersive and dissipative coupling is always about 10 ns shorter than that in the purely dissipative coupling case. For $\phi = \pi$, it is noted that the group delay $\tau_g(0)$ in the case of the combined dispersive and dissipative coupling is at most about 10 ns shorter than that in the purely dissipative coupling case. Therefore, in the critical coupling regime, the dispersive coupling has almost no effect on the intensity $|t_p(0)|^2$ of the output probe field, but it has a non-negligible impact on the group delay $\tau_g(0)$ of the output probe field. In the undercoupling regime ($\eta = 0.2$), when the power of the coupling field is $\mathcal{E}_c = 1 \mu\text{W}$, the steady-state mechanical displacement q_s is found to be about $-3.37 \times 10^{-14} \text{ m}$, which is very small, thus the approximations of $\omega_0(q)$ and $\kappa_c(q)$ in Eq. (2) are valid. Figure 14 shows the intensity $|t_p(0)|^2$ and group delay $\tau_g(0)$ of the output probe field against the amplitude parameter u of the mechanical drive when $\eta = 0.2$,

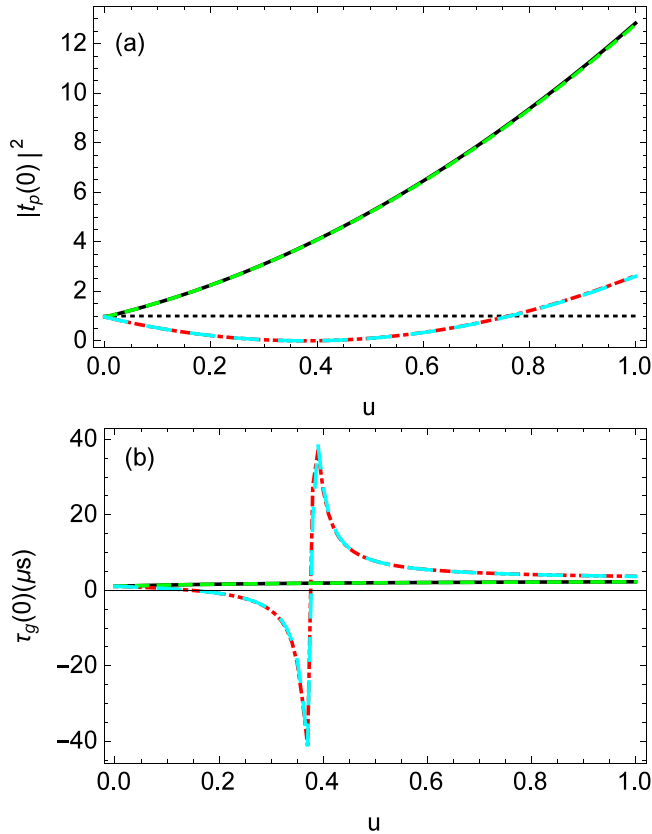


FIG. 14. The (a) intensity $|t_p(0)|^2$ and (b) group delay $\tau_g(0)$ of the output probe field as a function of the amplitude parameter u of the mechanical drive when $\eta = 0.2$, $\mathcal{E}_c = 1 \mu\text{W}$, and $\phi = 0, \pi$. The green short-dashed and cyan long-dashed curves correspond to the case of the combined dissipative and dispersive coupling, and they represent $\phi = 0$ and $\phi = \pi$, respectively. The black solid and red dot-dashed curves correspond to the case of the purely dissipative coupling, and they represent $\phi = 0$ and $\phi = \pi$, respectively. The flat dotted line in (a) represents $|t_p(0)|^2 = 1$.

$\mathcal{E}_c = 1 \mu\text{W}$, and $\phi = 0, \pi$. In Fig. 14(a), for $\phi = 0, \pi$, it is seen that the numerical results for the intensity $|t_p(0)|^2$ in the case of the combined dispersive and dissipative coupling are almost identical to those in the purely dissipative coupling case, respectively. In Fig. 14(b), for $\phi = 0, \pi$, it is seen that the curves for the group delay $\tau_g(0)$ in the case of the combined dispersive and dissipative coupling almost overlap those in the purely dissipative coupling case, respectively.

Therefore, the dispersive coupling barely affects the intensity $|t_p(0)|^2$ and group delay $\tau_g(0)$ of the output probe field in the undercoupling regime.

VI. CONCLUSIONS

In conclusion, we have investigated the propagation of a weak probe field in a waveguide-microdisk dissipative optomechanical system with a weak coherent mechanical drive. When a strong coupling field is present, we find that the probe field can be nearly totally absorbed, totally transmitted, and amplified by varying the amplitude and phase of the mechanical drive and the power of the coupling field in both the critical coupling regime and the undercoupling regime. We show that it is possible to achieve the EIT-like effect and the EIA-like effect in such a system. Moreover, we show that the group delay of the output probe field can be manipulated by controlling the amplitude and phase of the mechanical drive. Such control can even cause a switch from the slowing of the output probe field to the advancing of the output probe field and vice versa. Additionally, we compare the effects of the mechanical drive on the intensity and group delay of the output probe field in the optomechanical system with combined dispersive and dissipative coupling with those in the purely dissipative optomechanical system. For a certain range of system parameters, we find that the small dispersive optomechanical coupling in the experiment [15] has a negligible effect on the intensity of the output probe field in both the critical coupling regime and the undercoupling regime, and it also has a negligible effect on the group delay of the output probe field in the undercoupling regime, but it has a non-negligible influence on the group delay of the output probe field in the critical coupling regime. Therefore, this system can be used as an optical switch to control the propagation of a weak probe field in future quantum information networks [40].

ACKNOWLEDGMENTS

This work is supported by the National Natural Science Foundation of China under Grants No. 12174344, No. 12175199, and No. 91636108; the Zhejiang Provincial Natural Science Foundation of China under Grants No. LY21A040007 and No. LZ20A040002; and the Science Foundation of Zhejiang Sci-Tech University under Grant No. 17062071-Y.

- [1] M. Aspelmeyer, T. J. Kippenberg, and F. Marquardt, Cavity optomechanics, *Rev. Mod. Phys.* **86**, 1391 (2014).
- [2] G. S. Agarwal and S. Huang, Electromagnetically induced transparency in mechanical effects of light, *Phys. Rev. A* **81**, 041803(R) (2010).
- [3] S. Weis, R. Riviere, S. Deléglise, E. Gavartin, O. Arcizet, A. Schliesser, and T. J. Kippenberg, Optomechanically induced transparency, *Science* **330**, 1520 (2010).
- [4] A. H. Safavi-Naeini, T. P. Mayer Alegre, J. Chan, M. Eichenfield, M. Winger, Q. Lin, J. T. Hill, D. Chang, and

O. Painter, Electromagnetically induced transparency and slow light with optomechanics, *Nature (London)* **472**, 69 (2011).

- [5] X. Zhou, F. Hocke, A. Schliesser, A. Marx, H. Huebl, R. Gross, and T. J. Kippenberg, Slowing, advancing and switching of microwave signals using circuit nanoelectromechanics, *Nat. Phys.* **9**, 179 (2013).
- [6] P. Kharel, G. I. Harris, E. A. Kittlaus, W. H. Renninger, N. T. Otterstrom, J. G. E. Harris, and P. T. Rakich, High-frequency cavity optomechanics using bulk acoustic phonons, *Sci. Adv.* **5**, eaav0582 (2019).

- [7] K. J. Boller, A. Imamoglu, and S. E. Harris, Observation of electromagnetically induced transparency, *Phys. Rev. Lett.* **66**, 2593 (1991).
- [8] A. Kasapi, M. Jain, G. Y. Yin, and S. E. Harris, Electromagnetically induced transparency: Propagation dynamics, *Phys. Rev. Lett.* **74**, 2447 (1995).
- [9] M. Fleischhauer, A. Imamoglu, and J. P. Marangos, Electromagnetically induced transparency: Optics in coherent media, *Rev. Mod. Phys.* **77**, 633 (2005).
- [10] A. Lezama, S. Barreiro, and A. M. Akulshin, Electromagnetically induced absorption, *Phys. Rev. A* **59**, 4732 (1999).
- [11] F. Hocke, X. Zhou, A. Schliesser, T. J. Kippenberg, H. Huebl, and R. Gross, Electromechanically induced absorption in a circuit nano-electromechanical system, *New J. Phys.* **14**, 123037 (2012).
- [12] K. Qu and G. S. Agarwal, Phonon mediated electromagnetically induced absorption in hybrid opto-electro mechanical systems, *Phys. Rev. A* **87**, 031802(R) (2013).
- [13] V. Fiore, C. Dong, M. C. Kuzyk, and H. Wang, Optomechanical light storage in a silica microresonator, *Phys. Rev. A* **87**, 023812 (2013).
- [14] F. Elste, S. M. Girvin, and A. A. Clerk, Quantum noise interference and backaction cooling in cavity nanomechanics, *Phys. Rev. Lett.* **102**, 207209 (2009).
- [15] M. Li, W. H. P. Pernice, and H. X. Tang, Reactive cavity optical force on microdisk-coupled nanomechanical beam waveguides, *Phys. Rev. Lett.* **103**, 223901 (2009).
- [16] A. Sawadsky, H. Kaufer, R. M. Nia, S. P. Tarabrin, F. Ya. Khalili, K. Hammerer, and R. Schnabel, Observation of generalized optomechanical coupling and cooling on cavity resonance, *Phys. Rev. Lett.* **114**, 043601 (2015).
- [17] A. W. Barnard, M. Zhang, G. S. Wiederhecker, M. Lipson, and P. L. McEuen, Real-time vibrations of a carbon nanotube, *Nature (London)* **566**, 89 (2019).
- [18] A. G. Primo, P. V. Pinho, R. Benevides, S. Gröblacher, G. S. Wiederhecker, and T. P. M. Alegre, Dissipative optomechanics in high-frequency nanomechanical resonators, *Nat. Commun.* **14**, 5793 (2023).
- [19] A. Xuereb, R. Schnabel, and K. Hammerer, Dissipative optomechanics in a Michelson-Sagnac interferometer, *Phys. Rev. Lett.* **107**, 213604 (2011).
- [20] S. P. Tarabrin, H. Kaufer, F. Y. Khalili, R. Schnabel, and K. Hammerer, Anomalous dynamic backaction in interferometers, *Phys. Rev. A* **88**, 023809 (2013).
- [21] T. Weiss and A. Nunnenkamp, Quantum limit of laser cooling in dispersively and dissipatively coupled optomechanical systems, *Phys. Rev. A* **88**, 023850 (2013).
- [22] A. K. Tagantsev, Dissipative-coupling-assisted laser cooling: Limitations and perspectives, *Phys. Rev. A* **102**, 043520 (2020).
- [23] A. Karpenko and S. P. Vyatchanin, Combination of dissipative and dispersive coupling in the cavity optomechanical systems, *Phys. Rev. A* **105**, 063506 (2022).
- [24] M. Wu, A. C. Hryciw, C. Healey, D. P. Lake, H. Jayakumar, M. R. Freeman, J. P. Davis, and P. E. Barclay, Dissipative and dispersive optomechanics in a nanocavity torque sensor, *Phys. Rev. X* **4**, 021052 (2014).
- [25] J. G. Huang, Y. Li, L. K. Chin, H. Cai, Y. D. Gu, M. F. Karim, J. H. Wu, T. N. Chen, Z. C. Yang, Y. L. Hao, C. W. Qiu, and A. Q. Liu, A dissipative self-sustained optomechanical resonator on a silicon chip, *Appl. Phys. Lett.* **112**, 051104 (2018).
- [26] K. Qu and G. S. Agarwal, Generating quadrature squeezed light with dissipative optomechanical coupling, *Phys. Rev. A* **91**, 063815 (2015).
- [27] D. Kilda and A. Nunnenkamp, Squeezed light and correlated photons from dissipatively coupled optomechanical systems, *J. Opt.* **18**, 014007 (2016).
- [28] A. K. Tagantsev, I. V. Sokolov, and E. S. Polzik, Dissipative versus dispersive coupling in quantum optomechanics: Squeezing ability and stability, *Phys. Rev. A* **97**, 063820 (2018).
- [29] A. Karpenko, M. Korobko, and S. P. Vyatchanin, Enhanced optomechanical interaction in an unbalanced Michelson-Sagnac interferometer, *Phys. Rev. A* **108**, 053507 (2023).
- [30] S. Huang and G. S. Agarwal, Reactive coupling can beat the motional quantum limit of nanowaveguides coupled to a microdisk resonator, *Phys. Rev. A* **82**, 033811 (2010).
- [31] S. Huang and A. Chen, Mechanical squeezing in a dissipative optomechanical system with two driving tones, *Phys. Rev. A* **103**, 023501 (2021).
- [32] S. Huang and G. S. Agarwal, Reactive-coupling-induced normal mode splittings in microdisk resonators coupled to waveguides, *Phys. Rev. A* **81**, 053810 (2010).
- [33] T. Weiss, C. Bruder, and A. Nunnenkamp, Strong-coupling effects in dissipatively coupled optomechanical systems, *New J. Phys.* **15**, 045017 (2013).
- [34] W. Z. Jia, L. F. Wei, Y. Li, and Y.-X. Liu, Phase-dependent optical response properties in an optomechanical system by coherently driving the mechanical resonator, *Phys. Rev. A* **91**, 043843 (2015).
- [35] X.-W. Xu and Y. Li, Controllable optical output fields from an optomechanical system with mechanical driving, *Phys. Rev. A* **92**, 023855 (2015).
- [36] L. Fan, K. Y. Fong, M. Poot, and H. X. Tang, Cascaded optical transparency in multimode cavity optomechanical systems, *Nat. Commun.* **6**, 5850 (2015).
- [37] L.-G. Si, H. Xiong, M. S. Zubairy, and Y. Wu, Optomechanically induced opacity and amplification in a quadratically coupled optomechanical system, *Phys. Rev. A* **95**, 033803 (2017).
- [38] D. F. Walls and G. J. Milburn, *Quantum Optics* (Springer-Verlag, Berlin, 1998).
- [39] G. S. Agarwal and S. Huang, Nanomechanical inverse electromagnetically induced transparency and confinement of light in normal modes, *New J. Phys.* **16**, 033023 (2014).
- [40] H. J. Kimble, The quantum internet, *Nature (London)* **453**, 1023 (2008).